Heterogenous Profiles Between Matched Primary Tumors and Brain Metastases Reveal Tumor Evolution

Yanming Chen
Second Affiliated Hospital of Soochow University
Xiaoxiao Dai
Second Affiliated Hospital of Soochow University
Ji Wang
Second Affiliated Hospital of Soochow University
Chuming Tao
Second Affiliated Hospital of Soochow University
Ye Wang
Second Affiliated Hospital of Soochow University
Qing Zhu
Second Affiliated Hospital of Soochow University
Liqun Yuan
Second Affiliated Hospital of Soochow University
Zhongyong Wang
Second Affiliated Hospital of Soochow University
Minfeng Sheng
Second Affiliated Hospital of Soochow University
Tan Zhang
Second Affiliated Hospital of Soochow University
Shenggang Li
Second Affiliated Hospital of Soochow University
Yongsheng Zhang
Second Affiliated Hospital of Soochow University
Jun Dong
Second Affiliated Hospital of Soochow University
Qing Lan
Second Affiliated Hospital of Soochow University
Jizong Zhao (zhaojizong@bjtth.org)
Second Affiliated Hospital of Soochow University https://orcid.org/0000-0001-9194-0580

Research Article

Keywords: Heterogeneity, Brain metastasis, Lung cancer, Gene mutation, Evolution.

Posted Date: November 30th, 2021

DOI: https://doi.org/10.21203/rs.3.rs-1105667/v1

Abstract

Background: Brain metastases (BMs) are the most common central nervous system (CNS) malignant tumors, with rapid disease progression and extremely poor prognosis. The heterogeneity between primary tumors and BMs leads to the divergent efficacy of the adjuvant therapy response to primary tumors and BMs. However, the extent of heterogeneity between primary tumors and BMs, and the evolutionary process remains little known.

Methods: To deeply insight the extent of inter-tumor heterogeneity at single-patient level and the process of these evolutions, we retrospectively analyzed a total of 26 tumor samples from 11 patients with matched primary tumors and BMs. One patient underwent four times brain metastatic lesion surgery with diverse locations and one operation for the primary lesion. The genomic and immune heterogeneity between primary tumors and BMs was evaluated by utilizing the whole-exome sequencing (WESeq) and immunohistochemical analysis.

Results: In addition to inheriting genomic phenotype and molecular phenotype from the primary tumors, massive unique genomic phenotype and molecular phenotype were also observed in BMs, which revealed unimaginable complexity of tumor evolution and extensive heterogeneity among lesions at single-patient level. Our study also verified that the expression level of immune checkpoints-related molecule Programmed Death-Ligand 1 (PD-L1) ($P = 0.0013$) and the density of tumor-infiltrating lymphocytes (TILs) ($P = 0.0248$) in BMs were significantly lower than that in paired primary tumors. Additionally, tumor microvascular density (MVD) and tumor invasiveness were also differed between primary tumors and paired BMs, indicating that temporal and spatial diversity profoundly contributes to the evolution of BMs heterogeneity.

Conclusion: We verified the significance of temporal and spatial factors to the evolution of tumor heterogeneity by multi-dimensional analysis of matched primary tumors and BMs, which also provided novel insight for formulating individualized treatment strategies of BMs.

Introduction

Brain metastases (BMs) represent the most common type of malignant tumor in the central nervous system (CNS)(Cagney et al. 2017). The incidence of BMs has been increasing in recent years, due to the accumulated advances in the diagnostic and therapeutic strategy of primary tumors(Bachmann et al. 2015). Patients with BMs always suffered significantly worse prognostic outcomes(Meyers et al. 2004). The median survival time of patients with BMs leaves dismal only 5 weeks if no effective treatment(Svokos et al. 2014); while the survival time of patients with BMs can be prolonged to 3-18 months with valid treatment(Leibold et al. 2019).

BMs most commonly originate from lung cancer, breast cancer, renal cancer and melanoma(Gavrilovic and Posner 2005; Cagney et al. 2017). The survival of patients with BMs shared a gradual advance, with the improvements of BMs treatment in stereotactic radiosurgery (SRS)(Brown et al. 2016), neurosurgery(Al-Shamy and Sawaya 2009) and adjuvant therapies(Leone et al. 2020). In particular, immune checkpoint inhibitors and targeted therapy for specific mutations of cancer cells have become research focuses currently(Aquilanti and Brastianos 2020). However, accumulating evidence suggests that the special CNS microenvironment for metastatic tumor cells and the heterogeneity between primary tumors and BMs during the evolution often become critical obstacles leading to treatment failure(Leibold et al. 2019; Perus and Walsh 2019). The heterogeneity of BMs represents a severe challenge of precision medicine for BMs, which brings great difficulties to the individualized treatment of BMs(Kaidar-Person et al. 2018). To date, the extent of heterogeneity between BMs and primary tumors remains controversial, and the evolution of heterogeneity between BMs and primary tumors is largely unknown(De Bruin et al. 2014; Birkbak and McGranahan 2020). Furthermore, when regarding the question of the origin of metastases, whether monoclonal dissemination or polyclonal dissemination model? Which model is predominant in brain metastasis formation? The answer is still inconclusive(Brastianos et al. 2015; Noorani et al. 2020).

During the process of BMs formation, the shared molecular mechanism of the primary tumors plays its role, as well as the influence of CNS microenvironment on the disseminated tumor cells. It is hard to evaluate which side plays a prominent role. Though the long-standing dogma of “immune privilege” in CNS has been reconsidered in recent years(Herisson et al. 2018), its high immunosuppressive characteristic still being a serious obstacle to current tumor immunotherapy. In the past few years, immune checkpoint inhibitors have achieved great success in the treatment of lung cancer and melanoma. However, the effect of immune checkpoint inhibitors on BMs remains controversial(Schachter et al. 2017), and some clinical trials which included patients with BMs are underway. It has been reported that the expression level of PD-L1 in melanoma BMs was significantly lower than that of primary tumor and extracranial metastases(Leibold et al. 2019). This variability of PD-L1 expression and tumor-infiltrating lymphocytes (TILs) density between primary tumors and paired BMs may account for the variability in response to immune checkpoint inhibitors.

In this study, we comparative analyzed the data of capture-based WESeq and immunohistochemical profiles to assess the genomic heterogeneity, tumor driver genes and immune molecules variability between the primary tumors and paired BMs, based on paired analysis of a cohort of Primary-BMs samples. We expect deep insight into the extent of heterogeneity between primary tumors and BMs, and to explore the genomic and immunophenotypic heterogeneity evolutionary trajectory with multiple BMs that occurred at different spatial and temporal points at a single-patient level. Our study provides new insights for individualized treatment of BMs and gives us novel clues to the controversy over the model of metastatic dissemination.

Materials And Methods

Clinical samples

Eleven patients from the Second Affiliated Hospital of Soochow University (Suzhou, China) were included in our retrospective study from 2012 to 2020, with matched primary malignant tumors and BMs. These 11 patients all received primary tumor surgeries, one or more than one-time brain metastatic lesion

resections. Tumor tissues were obtained, formalin-fixed and paraffin-embedded (FFPE). Case 3 underwent 4 times divided brain metastatic lesion surgeries, spanning up to 54 months. A total of 26 tumor paraffin-embedded specimens were collected.

Whole exome sequencing and data processing

Genomic DNA from FFPE samples was extracted with GeneRead DNA FFPE Kit (180134, Qiagen, Germany). Genomic DNA samples were captured using Agilent SureSelect Human All Exon v6 library following the manufacturer's protocol (Agilent Technologies, USA). Briefly, approximately 3μg genomic DNA was sheared to 150 to 220bp small fragments using sonicator (Covaris, Inc., USA). The sheared DNA fragments were purified, and adapters from Agilent were ligated onto the polished ends and the libraries were amplified by polymerase chain reaction (PCR). The amplified libraries were hybridized with the custom probes. The DNA fragments bound with the probes were washed and eluted with the buffer. Then these libraries were sequenced on the Illumina sequencing platform (HiSeq X-10, Illumina, Inc., USA), 150bp paired-end reads were generated.

The raw reads were pre-processed with fastp (Version 0.19.5). Clean reads were aligned to the reference human genome (GRCh37) utilizing the BWA (Version 0.7.12). The mapped reads were sorted and indexed with SAMtools (Version 1.4). GATK (Version 4.1.0.0) was utilized for recalibration of the base quality score and single nucleotide polymorphism (SNP) and insertion/deletion (InDel) realignment. The frequency of SNP in 1000 Genomes Project or the Genome Aggregation Database (gnomAD) > 1% subpopulation were excluded. Copy number variation (CNV) was inferred from sequencing data using the software package CNVkit (Version 0.9.5), and Lumpy software (Version 0.2.13) was applied to call structural variation (SV). The detected genomic variation information was visualized using the Circos diagram. For shared mutations between primary tumors and brain metastatic tumors within each patient, we considered only 'D' level mutations of SIFT (sorts intolerant from tolerant) and Polyphen2_HDIV (Polymorphism Phenotyping v2) evaluation.

Histopathological analysis

All slices from the primary tumors and BMs of this cohort were independently diagnosed by two experienced pathologists. The immunohistochemical staining of EGFR (SP125, VENTANA, USA), PD-L1 (SP263, VENTANA, USA), CD34 (Kit-0004, MXB, China), CD4 (RMA-0620, MXB, China), CD8 (RMA-0514, MXB, China), ALK (D5F3, VENTANA, USA), MMP2 (40994, CST, USA) and MMP9 (13667, CST, USA) of FFPE followed the protocol. Microvascular density (MVD) of tumor tissue was assessed by a method published by Weidner(Weidner 1995).

Statistical analysis

GraphPad Prism (Version 8.0) was used for data analysis. Images were analyzed and recorded with Fiji (NIH open access, USA). The mean value differences were compared by analysis of variance (ANOVA). A paired Student's t-test was used to identify the difference between groups. A P-value 0.05 suggested statistical significance.

Results

Clinical characteristics of patients with primary lesions and paired BMs

The primary lesions of the 11 patients, included in our study (Table 1), were located in lung (7 cases), breast (1 case), kidney (1 case), stomach (1 case) and colon (1 case). All patients received primary tumors and BMs surgeries, and all tumor specimens were available. Therein, Case 3 underwent 4 times BMs surgeries within a time spanning up to 54 months (Figure 1A, B), and two independent brain metastatic specimens were obtained from Case 8. A cohort of 26 tumor specimens was analyzed (number of primary tumors and BMs, 11 vs. 15). The median overall survival time diagnosed with BMs was 22 months (range, 2-62 months). Traditionally, we share a viewpoint that the occurrence of BMs always represents the terminal stage of tumor development. However, recent studies implicated that the dissemination of primary tumors can occur at every stage of tumor progression(Birkbak and McGranahan 2020). This cohort of cases also supported the latter perspective. Part of the cases (4/11) developed disseminated BMs at the very early stage of lung cancer (Table 1). Those 4 patients first manifested as the symptoms of headache. The 4 patients underwent surgery for BMs, followed up receiving primary lesions surgery, with interval times 0.5 to 35 months. The remaining 7 patients all received the primary lesion surgery, and BMs emerged with different intervals when patients manifested as CNS clinical presentation, and the surgery of BMs resection followed. Additionally, there were no more than 3 intracranial metastatic lesions when deciding to perform BMs surgery.

Table 1
The clinical data of primary tumors and paired BMs.

Case No.	Exp.ID	Age (Years)[1]	Gender	Location		Interval time (Months)[2]	Treatment of primary lesion	Treatment of metastatic lesion	Pathology (Type)		OS(Months)
				Primary	Metastatic				Primary	Metastatic	
1	LC_001	60	M	Lung	Lt. Cerebellum	-35	Biopsy	Total resection	Poorly differentiated SC	AC	38
2	LC_002	58	M	Lung	Rt. Temporal lobe	11	Resection	Total resection	Poorly differentiated SC	SC	72
3	LC_003	57	M	Lung	Rt. Occipital lobe	-2	Resection	Total resection	ASC	AC	54
	LC_004	58			Lt. Occipital lobe	8		Total resection		AC	
	LC_005	60			Rt. Cerebellum	31		Total resection		AC	
	LC_006	61			Lt. Cerebellum	47		Total resection		AC	
4	BC_001	37	F	Breast	Rt. Cerebellum	41	Resection	Total resection	IDC	Poorly differentiated carcinoma	43
5	LC_007	44	F	Lung	Rt. Temporal parietal lobe	-15	Biopsy	Total resection	AC	Poorly differentiated AC	62
6	KC_001	51	M	Kidney	Rt. Frontal lobe	124	Resection	Total resection	CCRCC	Necrosis	146
7	LC_008	61	M	Lung	Lt. Frontal lobe	8	Resection	Total resection	Poorly differentiated AC	AC	37
8	LC_009	38	F	Lung	Subclavian lymph node	0	Resection	Biopsy	AC	AC	19
	LC_010	39			Lt. Frontal lobe	11		Total resection		AC	
	LC_011	39			Lt. Thalamus	11		Total resection		AC	
	LC_012	39			Subclavian lymph node	14		Biopsy		AC	
9	GC_001	48	M	Stomach	Lt. Occipital lobe	13	Biopsy	Total resection	AC	AC	23
10	CC_001	62	M	Colon	Lt. Frontal lobe	5	Resection	Total resection	Moderately differentiated AC/MUC	AC	13
11	LC_013	58	M	Lung	Lt. Occipital lobe	-0.5	Resection	Total resection	Poorly differentiated AC	AC	13

1 The age of onset, regardless of whether the primary lesion diagnosis prior, or earlier diagnosis of metastases.

2 The value is positive, if treatment of the primary lesion prior to metastases, otherwise the value is negative.

3 Preoperative treatment of brain metastases.

Abbreviations: OS. Overall survival; ASC. Adenosquamous carcinoma; AC. Adenocarcinoma; SC. Squamous carcinoma; IDC. invasive ductal carcinoma; CCRC cell carcinoma; MUC. mucinous carcinomas; RT. Radiotherapy; CT. Chemotherapy; D. Dead; A. Alive.

Genomic heterogeneity analysis of primary tumor and paired BMs

We completed a cohort of 11 paired primary lung tumors and BMs tumor tissues WESeq (Case 2, Case 3, Case 7 and Case 11) (Figure 1B). To assess the genomic variability, the genomic SNPs and InDels of the paired primary and brain metastatic lesions were compared. Consistent with the previous report(Burrell et al. 2013), primary tumors accumulated more genomic variation than BMs (Supplementary Figure 1A, B). Subsequently, we screened the mutation sites for deleterious and compared the primary lesion with 4 brain metastatic lesions in Case 3. We found that SNPs (including missense, stopgain and stoploss) and InDels (including framesShift, stopgain and stoploss) shared a remarkable diversity between the primary lesion and the four divided BMs (Figure 2A). The primary tumor accumulated more deleterious genomic variations (SNP and InDel) than the 4 spatial and temporal divided BMs in Case 3 (Figure 2B), and the shared SNPs and InDels between primary lung cancer and BMs gradually decreased with gone by (Figure 1B and Figure 3A). We also found that compared with the primary tumor, only a small part of SNPs and InDels (ranging from 5.85% in Case 3_M4 to 38.78% in Case 11) (Figure 2C) were shared in BMs. Figure 3B summarized the frequency spectrum of common driver gene mutations. MUC16, PRX and SDHA showed the highest frequency of deleterious mutations, occurring in all primary lung cancers and BMs. It has been reported that the classic tumor marker CA125 encoded by the MUC16 gene played a vital role in regulating tumor cell metastasis(lei et al. 2020), and succinate dehydrogenase (SDH) complex subunits mutations were reported highly associated with tumor cells metastases in pheochromocytoma and paraganglioma and other malignancies(Gill 2018; Lee et al. 2020a).
Additionally, CDKN2A/B genes, a set of recognized lung cancer suppressor genes, copy number amplification were observed in M1, M3 and M4 BMs of Case 3, while no aberrations were found in the primary tumor and M2 (Figure 3C). It has been reported that STK11 and KEAP1 mutations were associated with poor prognosis in patients diagnosed with lung adenocarcinoma(Papillon-Cavanagh et al. 2020). Our study also indicated that STK11 and KEAP1 copy number deletions occurred in Case 3 and Case 7, but not all BMs in Case 3 were consistent (Figure 3C). Moreover, CNV events of a cohort of genes, including KRAS, CDKN2A/B and IDH1, were frequently found in brain metastatic lesions (Figure 3C). Supplementary Figure 2 summarized the total genomic fragments copy number aberrations, and common lung cancer- and brain tumor-related genes CNVs were marked. Integrated analysis of the genomic variation of the patient's primary tumors and BMs, we found that the genomic heterogeneity between the primary tumors and BMs was striking higher than we expected (Figure 3 and Supplementary Figure 2). The Circos diagram revealed that Case 3_M2 showed a significantly higher frequency of chromosomal aberrations (Supplementary Figure 2B), such as interchromosomal translocations. The analysis of cancer cells' clonal composition in BMs revealed a similar clonal clusters composition in Case 3, with the characteristics of polyclonal dissemination (Figure 4A, B).

Internal histopathologic heterogeneity and evolution analysis

In most cases, the histomorphological differences between the primary lung tumors and BMs were limited (Figure 5A and Supplementary Figure 3B-D). However, we still observed some alterations in Case 3 with multiple recurrences. From foci M1 to M4, it showed a variable level of cancer cell differentiation, from well-differentiated to poorly differentiated. Metastatic lesions still basically maintained the histopathological characteristics of the primary lung cancer at an early stage of dissemination. However, we found a remarkably poorer degree of tumor differentiation in the extremely long-term brain metastatic foci than the primary lesion, with the classic tube-like structure gradually disappeared. Tumor cell clusters were diffusely distributed, and the nucleus atypia, mitosis and giant polymorphic nucleus could be observed frequently in metastatic foci M4 (Figure 5A).

Tumor-related immune heterogeneity between primary lesions and paired BMs

Emerging evidence suggests that brain is not an "immune privileged" organ as previously thought. The immune checkpoint therapy targeting the PD1/PD-L1 pathway has notably improved the survival outcomes of several types of malignant tumors, which also brought hope to patients with BMs. Higher PD-L1 expression of tumor cells and/or TILs density is always associated with favorable anti-PD1/PD-L1 immunotherapeutic efficacy(Ribas and Hu-Lieskovan 2016). However, in contrast with the primary lesions, the efficacy of immune checkpoint therapy targeting PD1/PD-L1 in BMs is indeed not so significant(Goldberg et al. 2016; Kluger et al. 2019). Herein, we assessed PD-L1 expression in a cohort of primary tumors and paired BMs by immunohistochemistry. Our study indicated that the expression level of PD-L1 in metastatic tumor cells was significantly lower than that of paired primary lung cancers ($P = 0.0013$) (Figure 5).

TILs, especially CD8+ TILs, represent a favorable prognostic factor in several types of cancers(Gueguen et al. 2021). Meanwhile, CD8+ TILs performed as the final executor of PD1/PD-L1 pathway. A comparative study on primary tumors and paired metastases revealed that the density of CD8+ TILs in BMs was significantly lower than that of matched primary tumors ($P = 0.0248$) (Figure 6A-C). Our results also demonstrated a relatively lower density of CD4+ T cells in primary lung cancers (Case 2, 3, 7 and 11) and paired BMs, while the density of CD4+ T cells was higher in breast cancer (Case 4) and colorectal cancer (Case 10) (Supplementary Figure 4A, B). Although only Case 11 was treated with PD1/PD-L1 blockade immunotherapies in this cohort of retrospective study, the above analysis still benefits us to comprehensively insight the immune microenvironment of BMs, provides us novel clues to evaluate the efficacy of immunotherapy of BMs. In summary, BMs differed from paired primary tumors by showing notable immunosuppressive characteristics than primary tumors.

Analysis of immunohistochemical phenotypic heterogeneity between primary lesions and paired BMs

Finally, we integrative analyzed the molecular phenotypes of all 11 primary tumors and paired BMs. Although primary tumors and paired BMs shared pivotal molecular phenotypes, such as the EGFR expression and EML4-ALK fusion status in lung cancer cases (Case 2, Case 3, Case 7 and Case 11), ER, PR, and HER2 expression status in Case 4 (Supplementary Figure 3 and Supplementary Table 1). While comparatively analyzed tumor invasiveness (MMP2 and MMP9 staining) and tumor microvascular density (MVD) (CD34 staining), a notable difference of MVD was found between the primary tumors and paired BMs, and inter-BMs, with tumor MVD more plentiful in BMs than in the paired primary tumors (Figure 7A-C and Supplementary Figure 5A). Meanwhile, the expression of MMP2 and MMP9 in primary tumors was significantly higher than that in metastatic tumors (Supplementary Figure 5B, C).

Discussion

Traditionally, the occurring of BMs always represents the end-product of tumor progression, but some researchers believe that the dissemination of primary tumor cells can occur at various stages of tumor progression(Hu et al. 2019; Birkbak and McGranahan 2020). Our result from a cohort of matched primary tumors and BMs cases tended to support the latter perspective, a proportion of patients (4/11) developed disseminated brain tumors before primary tumor resection, or parallel with primary tumor evolution. Although we have been warned that intra-tumors genetic heterogeneity was extensive, has long been believed that the phenotypic heterogeneity may not be so extensive, especially between the primary and metastatic lesions at single-patient level. We ignored that, though the shared molecular mechanism in primary tumor played an important role, the influence of CNS microenvironment exerted on the disseminated tumor cells during BMs formation was equally vital(Winkler 2015). The selective pressure from the brain microenvironment on the disseminated tumor cells and the inherent heterogeneity within the primary tumor are responsible for the significant difference between primary tumor and metastatic lesion at single-patient level, and this heterogeneity may derive from the tumor branching evolution. By comparative analyzing a cohort of matched primary tumor and BMs cases (some cases received multiple BMs surgeries), we expected to exploit the role of spatial and temporal factors in the evolution of tumor heterogeneity. The heterogeneity between primary tumors and metastatic lesions, which occurred at different times and spaces, can also reveal tumor evolution at single-patient level(De Bruin et al. 2014). Briefly, it is helpful for us to deep insight into the molecular genetics of tumor dissemination and metastasis by a comprehensive understanding of the evolutionary dynamics of tumor progression.

Herein, based on the results of WESeq, we first exhibited a cohort of matched primary tumors and BMs deleterious genomic SNPs and InDels evolution landscape. The results demonstrated that the shared mutations of lung cancer driver genes between the primary lung cancers and the BMs gradually decreased as time goes on, though the difference lacked statistical significance due to the limited number of cases. Subsequent CNV analysis of lung cancer- and brain tumor-associated driver genes found that there was also widespread heterogeneity between the primary tumors and BMs, even without a shared CNV event in the multi-metastases case (Case 3). CDKN2A/B, STK11 and KEAP1 had a high frequency of alterations in lung cancer BMs cases. Noteworthy, the alterations of CDKN2A/B in three BMs showed copy number amplification in Case 3, instead of CNV deletion reported(Young et al. 2014; Wang et al. 2019).

When regarding the origin of metastasis, there have always been two hypotheses, monoclonal dissemination and polyclonal dissemination from primary tumors(Birkbak and McGranahan 2020). Echoing previous studies(Brown et al. 2017; De Mattos-Arruda et al. 2019), we found that primary tumors accumulated more genomic aberrations than BMs. There was also considerable heterogeneity among metastatic lesions at single-patient level, which tended to support the hypothesis of polyclonal dissemination.

In all types of metastatic tumors, a common feature in each step of tumor cell dissemination is the need to escape recognition and destruction by the immune system(Leibold et al. 2019). This immune escape mechanism plays an important role in the formation of BMs. We analyzed the molecular phenotypes of immune checkpoint between primary lesions and paired BMs and found that PD-L1 was highly expressed in primary lesions, while the expression of PD-L1 in metastatic lesions was significantly lower than that of matched primary lung tumors. Moreover, our study also found that the density of CD8+ TILs in BMs was remarkably lower than matched primary tumors. All our results suggested that BMs showed the characteristic of immunosuppression. This clue also partly confirmed the current dilemma of immunotherapy of BMs. Immune checkpoint inhibitors seem to be less effective on BMs than primary tumors(Dudnik et al. 2016; Aquilanti and Brastianos 2020). The causes of extensive immune-associated phenotypic heterogeneity between primary tumors and BMs may various(Lee et al. 2020b). One possible factor, that the unique immunosuppressive characteristics of CNS microenvironment may shape clonal metastatic cancer genome evolution, cannot be ignored (Angelova et al. 2018; Birkbak and McGranahan 2020). However, our study also has some limitations. First, due to a retrospective study, matched germline DNA of patients as normal controls were not available, and lack of more suitable samples for further transcriptomic and proteomic analysis, which may provide more accurate details for the evolution of BMs heterogeneity from peripheral malignant tumors. Additionally, restricted by the number of matched primary tumors and BMs, the statistical analysis of results is difficult. To verify our hypothesis, we need to accumulate more detailed matched primary tumors and BMs cases in further research, by combining with single-cell sequencing, to deeply analyze the role of the CNS microenvironment in shaping BMs.

Conclusion

In summary, our retrospective analysis results shed light upon the significant heterogeneity between matched primary tumors and BMs, and the complexity of the evolutionary process, especially the evolutionary process of heterogeneity due to temporal and spatial dynamic changes at single-patient level. And our results verified the characteristic of immunosuppressive in BMs, which also provide novel insight for formulating individualized treatment strategies of BMs.

Declarations

Acknowledgements

Not applicable

Data Availability Statement

All data presented in this study are available from the correspondent for reasonable request.

Author contributions

Yanming Chen and Xiaoxiao Dai designed this study. Xiaoxiao Dai and Yongsheng Zhang were responsible for pathological diagnosis and immunohistochemical experiments. Ji Wang, Qing Zhu, Liqun Yuan, Ye Wang, Minfeng Sheng, Zhongyong Wang and Tan Zhang supported and analyzed clinical data. Jizong Zhao and Qing Lan guided this work and reviewed the manuscript. All authors approved the final version of the submitted manuscript.

Funding

Our work presented above, was funded by the National Natural Science Foundation of China (81602183), the Youth Medical Talent Foundation of Jiangsu (QNRC2016870) and the Project of Suzhou Health Talents (2020090).

Conflict of Interest

The authors declare that the research was conducted in the absence of any commercial or financial relationships that could be construed as a potential conflict of interest.

Ethics statement

All participants provided informed consent. The study was approved by the ethics committee of The Second Affiliated Hospital of Soochow University.

Informed consent

Not applicable

References

1. Al-Shamy G, Sawaya R (2009) Management of brain metastases: the indispensable role of surgery. J Neurooncol 92:275–282. https://doi.org/10.1007/s11060-009-9839-y
2. Angelova M, Mlecnik B, Vasaturo A, et al (2018) Evolution of Metastases in Space and Time under Immune Selection. Cell 175:751-765.e16. https://doi.org/10.1016/j.cell.2018.09.018
3. Aquilanti E, Brastianos PK (2020) Immune checkpoint inhibitors for brain metastases: A primer for neurosurgeons. Neurosurgery 87:E281–E288. https://doi.org/10.1093/neuros/nyaa095
4. Bachmann C, Schmidt S, Staebler A, et al (2015) CNS metastases in breast cancer patients: prognostic implications of tumor subtype. Med Oncol 32:400. https://doi.org/10.1007/s12032-014-0400-2
5. Birkbak NJ, McGranahan N (2020) Cancer Genome Evolutionary Trajectories in Metastasis. Cancer Cell 37:8–19. https://doi.org/10.1016/j.ccell.2019.12.004
6. Brastianos PK, Carter SL, Santagata S, et al (2015) Genomic Characterization of Brain Metastases Reveals Branched Evolution and Potential Therapeutic Targets. Cancer Discov 5:1164–1177. https://doi.org/10.1158/2159-8290.CD-15-0369
7. Brown D, Smeets D, Székely B, et al (2017) Phylogenetic analysis of metastatic progression in breast cancer using somatic mutations and copy number aberrations. Nat Commun 8:14944. https://doi.org/10.1038/ncomms14944
8. Brown PD, Jaeckle K, Ballman K V., et al (2016) Effect of Radiosurgery Alone vs Radiosurgery With Whole Brain Radiation Therapy on Cognitive Function in Patients With 1 to 3 Brain Metastases. JAMA 316:401. https://doi.org/10.1001/jama.2016.9839
9. Burrell RA, McGranahan N, Bartek J, Swanton C (2013) The causes and consequences of genetic heterogeneity in cancer evolution. Nature 501:338–345. https://doi.org/10.1038/nature12625
10. Cagney DN, Martin AM, Catalano PJ, et al (2017) Incidence and prognosis of patients with brain metastases at diagnosis of systemic malignancy: a population-based study. Neuro Oncol 19:1511–1521. https://doi.org/10.1093/neuonc/nox077
11. De Bruin EC, McGranahan N, Mitter R, et al (2014) Spatial and temporal diversity in genomic instability processes defines lung cancer evolution. Science (80-) 346:251–256. https://doi.org/10.1126/science.1253462
12. De Mattos-Arruda L, Sammut S-J, Ross EM, et al (2019) The Genomic and Immune Landscapes of Lethal Metastatic Breast Cancer. Cell Rep 27:2690-2708.e10. https://doi.org/10.1016/j.celrep.2019.04.098
13. Dudnik E, Yust-Katz S, Nechushtan H, et al (2016) Intracranial response to nivolumab in NSCLC patients with untreated or progressing CNS metastases. Lung Cancer 98:114–117. https://doi.org/10.1016/j.lungcan.2016.05.031
14. Gavrilovic IT, Posner JB (2005) Brain metastases: epidemiology and pathophysiology. J Neurooncol 75:5–14. https://doi.org/10.1007/s11060-004-8093-6
15. Gill AJ (2018) Succinate dehydrogenase (SDH)-deficient neoplasia. Histopathology 72:106–116. https://doi.org/10.1111/his.13277
16. Goldberg SB, Gettinger SN, Mahajan A, et al (2016) Pembrolizumab for patients with melanoma or non-small-cell lung cancer and untreated brain metastases: early analysis of a non-randomised, open-label, phase 2 trial. Lancet Oncol 17:976–983. https://doi.org/10.1016/S1470-2045(16)30053-5

17. Gueguen P, Metoikidou C, Dupic T, et al (2021) Contribution of resident and circulating precursors to tumor-infiltrating CD8 + T cell populations in lung cancer. Sci Immunol 6:eabd5778. https://doi.org/10.1126/sciimmunol.abd5778
18. Herisson F, Frodermann V, Courties G, et al (2018) Direct vascular channels connect skull bone marrow and the brain surface enabling myeloid cell migration. Nat Neurosci 21:1209–1217. https://doi.org/10.1038/s41593-018-0213-2
19. Hu Z, Ding J, Ma Z, et al (2019) Quantitative evidence for early metastatic seeding in colorectal cancer. Nat Genet 51:1113–1122. https://doi.org/10.1038/s41588-019-0423-x
20. Kaidar-Person O, Meattini I, Jain P, et al (2018) Discrepancies between biomarkers of primary breast cancer and subsequent brain metastases: an international multicenter study. Breast Cancer Res Treat 167:479–483. https://doi.org/10.1007/s10549-017-4526-8
21. Kluger HM, Chiang V, Mahajan A, et al (2019) Long-Term Survival of Patients With Melanoma With Active Brain Metastases Treated With Pembrolizumab on a Phase II Trial. J Clin Oncol 37:52–60. https://doi.org/10.1200/JCO.18.00204
22. Lee H, Jeong S, Yu Y, et al (2020a) Risk of metastatic pheochromocytoma and paraganglioma in SDHx mutation carriers: a systematic review and updated meta-analysis. J Med Genet 57:217–225. https://doi.org/10.1136/jmedgenet-2019-106324
23. Lee WC, Reuben A, Hu X, et al (2020b) Multiomics profiling of primary lung cancers and distant metastases reveals immunosuppression as a common characteristic of tumor cells with metastatic plasticity. Genome Biol 21:1–21. https://doi.org/10.1186/s13059-020-02175-0
24. lei Y, Zang R, Lu Z, et al (2020) ERO1L promotes IL6/sIL6R signaling and regulates MUC16 expression to promote CA125 secretion and the metastasis of lung cancer cells. Cell Death Dis 11:853. https://doi.org/10.1038/s41419-020-03067-8
25. Leibold AT, Monaco GN, Dey M (2019) The role of the immune system in brain metastasis. Curr Neurobiol
26. Leone JP, Emblem KE, Weitz M, et al (2020) Phase II trial of carboplatin and bevacizumab in patients with breast cancer brain metastases. Breast Cancer Res 22:131. https://doi.org/10.1186/s13058-020-01372-w
27. Meyers CA, Smith JA, Bezjak A, et al (2004) Neurocognitive Function and Progression in Patients With Brain Metastases Treated With Whole-Brain Radiation and Motexafin Gadolinium: Results of a Randomized Phase III Trial. J Clin Oncol 22:157–165. https://doi.org/10.1200/JCO.2004.05.128
28. Noorani A, Li X, Goddard M, et al (2020) Genomic evidence supports a clonal diaspora model for metastases of esophageal adenocarcinoma. Nat Genet 52:74–83. https://doi.org/10.1038/s41588-019-0551-3
29. Papillon-Cavanagh S, Doshi P, Dobrin R, et al (2020) STK11 and KEAP1 mutations as prognostic biomarkers in an observational real-world lung adenocarcinoma cohort. ESMO Open 5:1–6. https://doi.org/10.1136/esmoopen-2020-000706
30. Perus LJM, Walsh LA (2019) Microenvironmental Heterogeneity in Brain Malignancies. Front Immunol 10:. https://doi.org/10.3389/fimmu.2019.02294
31. Ribas A, Hu-Lieskovan S (2016) What does PD-L1 positive or negative mean? J Exp Med 213:2835–2840. https://doi.org/10.1084/jem.20161462
32. Schachter J, Ribas A, Long G V, et al (2017) Pembrolizumab versus ipilimumab for advanced melanoma: final overall survival results of a multicentre, randomised, open-label phase 3 study (KEYNOTE-006). Lancet 390:1853–1862. https://doi.org/10.1016/S0140-6736(17)31601-X
33. Svokos K, Salhia B, Toms S (2014) Molecular Biology of Brain Metastasis. Int J Mol Sci 15:9519–9530. https://doi.org/10.3390/ijms15069519
34. Wang H, Ou Q, Li D, et al (2019) Genes associated with increased brain metastasis risk in non–small cell lung cancer: Comprehensive genomic profiling of 61 resected brain metastases versus primary non–small cell lung cancer (Guangdong Association Study of Thoracic Oncology 1036). Cancer 125:3535–3544. https://doi.org/10.1002/cncr.32372
35. Weidner N (1995) Current pathologic methods for measuring intratumoral microvessel density within breast carcinoma and other solid tumors. Breast Cancer Res Treat 36:169–180. https://doi.org/10.1007/BF00666038
36. Winkler F (2015) The brain metastatic niche. J Mol Med 93:1213–1220. https://doi.org/10.1007/s00109-015-1357-0
37. Young RJ, Waldeck K, Martin C, et al (2014) Loss of CDKN2A expression is a frequent event in primary invasive melanoma and correlates with sensitivity to the CDK4/6 inhibitor PD0332991 in melanoma cell lines. Pigment Cell Melanoma Res 27:590–600. https://doi.org/10.1111/pcmr.12228

Figures

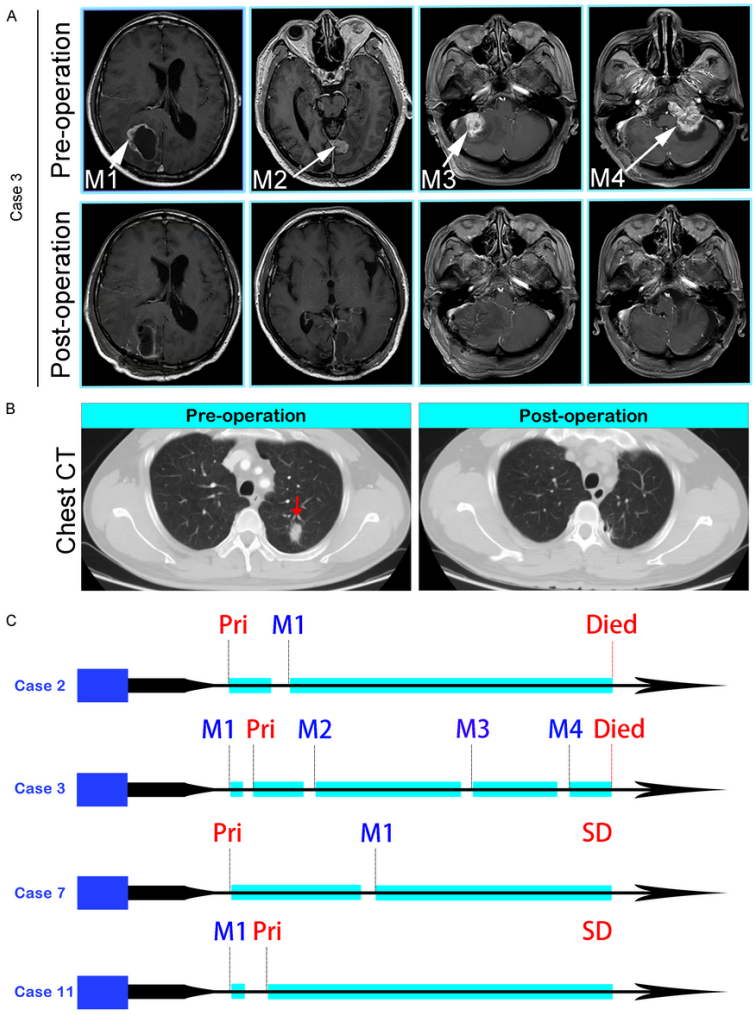

Figure 1

(A) MR images of four spatial and temporal divided BMs in Case 3, before (the upper panel) and after (the lower panel) surgeries. (B) CT imaging revealed an isolated lung lesion (Red arrow), and postoperative chest CT showed the lesion was removed totally. (C) Disease progression and treatment timelines of Case2, Case 3, Case 7 and Case 11. Abbreviations: Pri. Primary lung tumor; SD. Stable Disease.

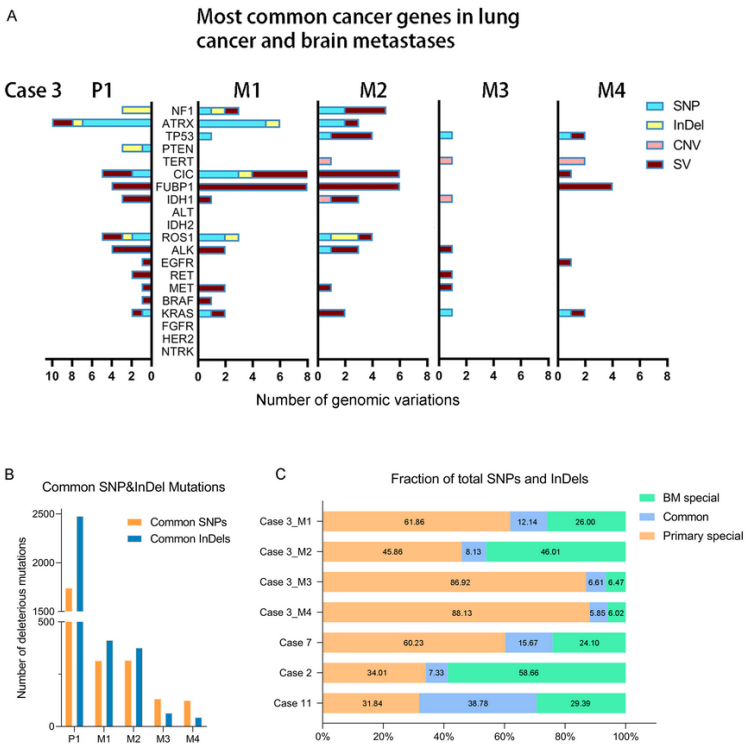

Figure 2

(A) The distribution of common lung cancer- and brain tumor-associated cancer gene genomic variations in primary tumor and different BMs of Case 3. (B) The distribution of the common SNP and InDel mutations between primary lung cancer and four BMs in Case 3. (C) The shared deleterious SNP and InDel may be varied between the primary lung cancer and paired BMs.

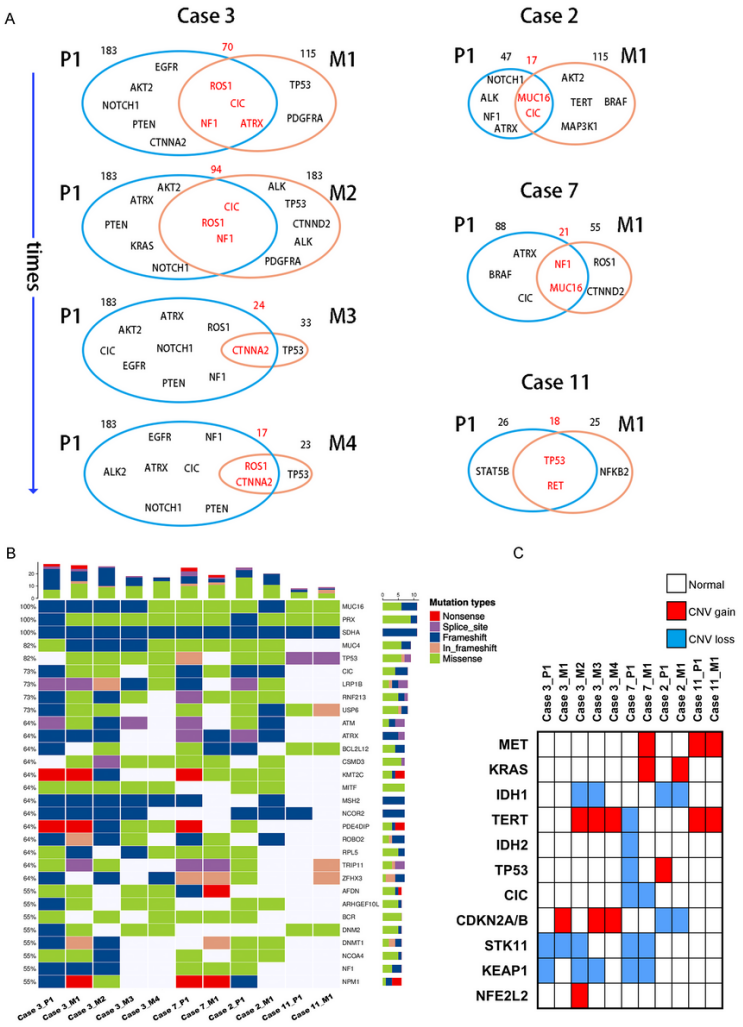

Figure 3

(A) Venn diagram exhibits the genetic concordance (SNP and InDel) between the primary lung tumors and paired BMs. (B) Heatmap of the top 30 common tumor driver genes mutations. (C) Heatmap shows common lung cancer- and brain tumor-associated cancer genes copy number variation in the primary lung tumors and paired BMs.

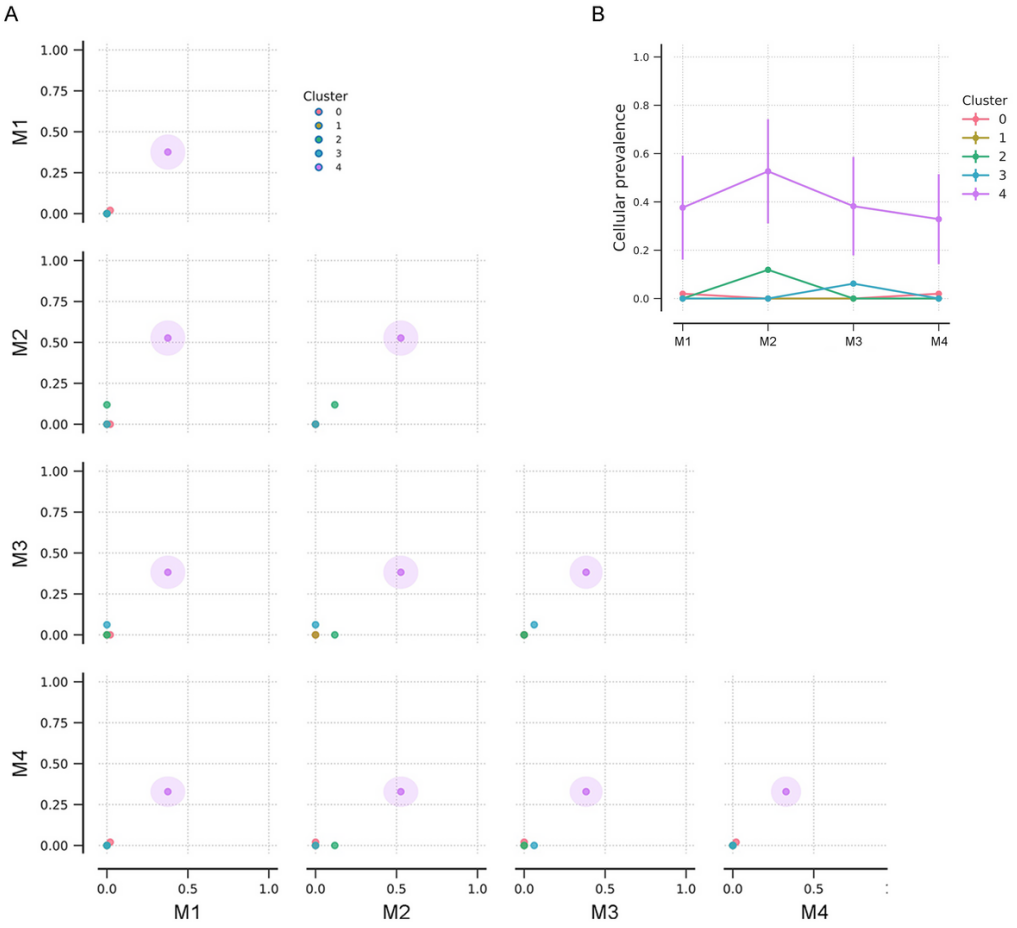

Figure 4

(A) The cluster correlation between samples of BMs in Case3. (B) The cellular prevalence of each cluster in the BMs of Case 3.

Figure 5

(A) H&E staining (the left panel) and PD-L1immunohistochemical staining (the right panel) of primary lung cancer and BMs in Case 3. The blue arrow in the magnified image points to the nucleus with apparent atypia. (B, C) PD-L1 immunohistochemical staining of primary lung cancers and BMs in Case 2 and Case 7, respectively. (D) Quantification of PD-L1 expression in each primary tumor and paired BMs. Scale bar = 100μm

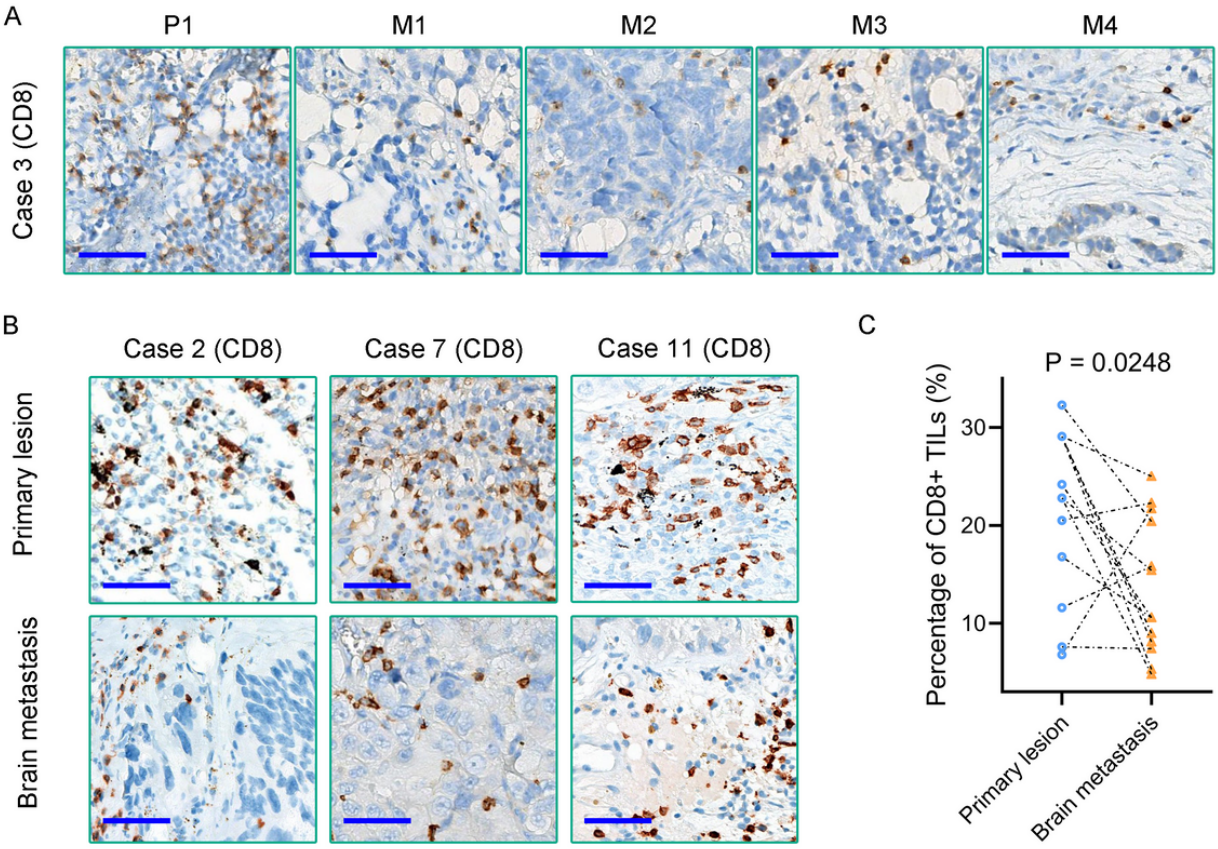

Figure 6

(A, B) Immunohistochemical staining reveals the density of CD8+ TILs in matched primary lung tumor and BMs; (C) Quantification of CD8+ TILs density in each primary tumor and paired BMs. Scale bar = 50μm

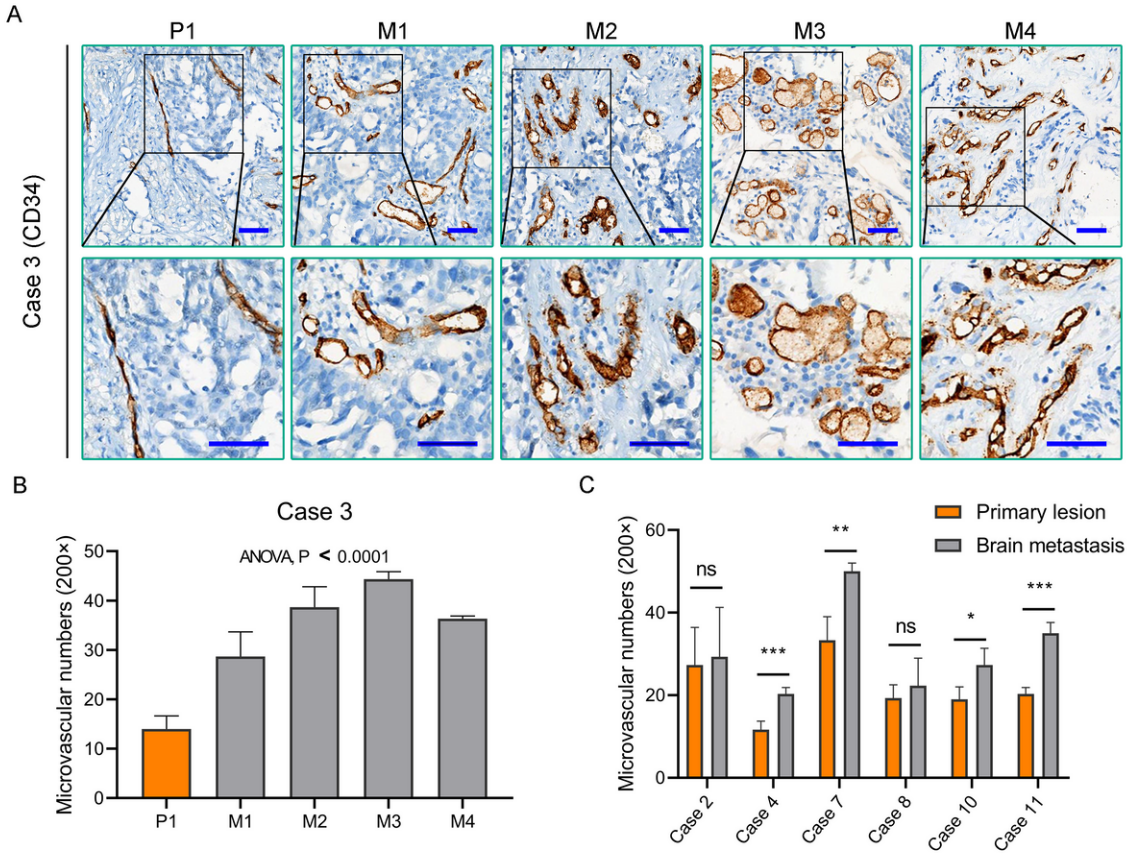

Figure 7

(A) CD34 immunohistochemical staining evaluates the heterogeneity of MVD between primary tumor and BMs in Case 3, the lower panel is the magnified images of the black frames (the upper panel). (B) Quantification of MVD in different lesions of Case 3. (C) Comparison of MVD between matched primary tumors and BMs. Scale bar = 50μm; * represent P ≤ 0.05; ** represent P ≤ 0.01; *** represent P ≤ 0.005; ns: not significant.

Supplementary Files

This is a list of supplementary files associated with this preprint. Click to download.

- FigureS1.png
- FigureS2.png
- FigureS3.png
- FigureS4.png
- FigureS5.png